

Cai-Hong Yun,<sup>a</sup> Juan Bai,<sup>b</sup>  
Da-Ye Sun,<sup>b</sup> Da-Fu Cui,<sup>c</sup>  
Wen-Rui Chang<sup>a</sup> and  
Dong-Cai Liang<sup>a\*</sup>

<sup>a</sup>National Laboratory of Biomacromolecules, Institute of Biophysics, Chinese Academy of Sciences, Beijing 100101, People's Republic of China, <sup>b</sup>Biology Department, Hebei Normal University, Shijiazhuang, Hebei Province 050016, People's Republic of China, and <sup>c</sup>Institute of Biochemistry and Cell Biology, Chinese Academy of Sciences, Shanghai 200031, People's Republic of China

Correspondence e-mail:  
dcliang@sun5.ibp.ac.cn

## Structure of potato calmodulin PCM6: the first report of the three-dimensional structure of a plant calmodulin

The crystal structure of a potato calmodulin (PCM6) was solved by molecular replacement and refined to a crystallographic  $R$  factor of 22.8% ( $R_{\text{free}} = 25.0\%$ ) using X-ray diffraction data in the resolution range 8.0–2.0 Å. This is the first report of the three-dimensional structure of a plant  $\text{Ca}^{2+}$ -calmodulin. PCM6 crystallizes in a crystal form that belongs to space group  $P2_12_12_1$ , which is different to that of most other calmodulin crystals. The main structural difference between PCM6 and the other calmodulins is in the central helix region and appears to be caused by crystal packing. The surface properties of PCM6 molecules were compared with those of animal calmodulins, which provided an explanation for the unique crystal-packing state of PCM6.

Received 31 December 2003  
Accepted 21 April 2004

**PDB Reference:** potato calmodulin PCM6, 1rfj, r1rfjsf.

### 1. Introduction

Calmodulin (CaM) is a ubiquitous multifunctional  $\text{Ca}^{2+}$  signal receptor in eukaryotes that participates in most of the important signalling pathways in cells (James *et al.*, 1995). It plays a key role in transducing  $\text{Ca}^{2+}$  signals to different physiological effects. In order to elucidate the functional mechanism of calmodulin, structural biological studies have been undertaken on several kinds of calmodulins and calmodulin complexes from animals and *Paramecium tetraurelia* (Babu *et al.*, 1985, 1988; Ban *et al.*, 1994; Chattopadhyaya *et al.*, 1992; Drum *et al.*, 2002; Elshorst *et al.*, 1999; Ikura, Kay *et al.*, 1991; Ikura, Spera *et al.*, 1991; Ikura, Barbato *et al.*, 1992; Ikura, Clore *et al.*, 1992; Kurokawa *et al.*, 2001; Meador *et al.*, 1992; Osawa *et al.*, 1999; Rao *et al.*, 1993; Schumacher *et al.*, 2001; Taylor *et al.*, 1991; Wilson & Brünger, 2000), but there has not been any report of the three-dimensional structure of a plant calmodulin. Although plant CaMs are similar to animal CaMs in amino-acid sequence and function, there are also some differences (Zielinski, 1998): several sites in the amino-acid sequences of higher plant CaMs have been found to be typically different from those of animal CaMs (Fig. 1). There are usually several types of CaM isomer in a single higher plant species, while animal species generally expresses only one type of CaM. There are also subtle differences between plant CaMs and animal CaMs in the types and properties of the target proteins of CaM. Since there is no report of the three-dimensional structure of a plant CaM, it remains unclear whether plant CaMs are the same as other CaMs in structure and mechanism.

PCM6 is one of the six CaM isomers in potato (*Solanum tuberosum*). Since its amino-acid sequence is typical of that of plant CaMs (Fig. 1), its three-dimensional structure and functional mechanism should be representative.

## 2. Materials and methods

### 2.1. Expression and purification of PCM6

The plasmid (pET32b) containing the potato calmodulin gene PCM6 was kindly provided by Professor Poovaiah (Laboratory of Plant Molecular Biology and Physiology, Department of Horticulture, Washington State University, USA). The *Escherichia coli*-expressed PCM6 protein was primarily purified using a phenyl-Sepharose column according to the method of Biro *et al.* (1984) and then was further purified to achieve the purity for crystallization using a Mono-Q anion ion-exchange column (0–1 M NaCl, 20 mM Tris pH 8.5, 2 mM EGTA) and a Superdex 75 gel-filtration column (20 mM Tris pH 8.0, 1 mM CaCl<sub>2</sub>, 0.1 M NaCl).

### 2.2. Crystallization and data collection

PCM6 was crystallized by the hanging-drop vapour-diffusion method at 277 K. The reservoir solution was 1.0 ml 45% (v/v) MPD, 5 mM CaCl<sub>2</sub>, 0.1 M sodium acetate/acetic acid pH 3.90. The hanging-drop solution was made by mixing 2 µl reservoir solution with 2 µl 16 mg ml<sup>-1</sup> PCM6 protein solution. Crystals as large as 1.2 × 0.4 × 0.03 mm were obtained in about one month.

A data set diffracting to 2.0 Å was collected at 100 K on beamline BL6B of the Tsukuba Photon Factory. The space group was *P*<sub>2</sub><sub>1</sub><sub>2</sub><sub>1</sub><sub>2</sub><sub>1</sub>, with unit-cell parameters *a* = 24.4, *b* = 69.0, *c* = 109.9 Å. The data were processed and scaled with *DENZO*

**Table 1**

Data set and refinement statistics.

Values in parentheses are for the highest resolution shell (2.05–2.00 Å).	
Data processing	
Resolution limit (Å)	2.0
Total reflections	108487
Unique reflections	12583
Completeness (%)	95.1 (88.9)
<i>I</i> / $\sigma$ ( <i>I</i> )	23.5 (6.1)
<i>R</i> <sub>merge</sub>	0.056 (0.129)
Refinement statistics	
Resolution (Å)	8.0–2.0
No. non-H protein atoms	1161
No. Ca <sup>2+</sup> ions	4
No. non-H MPD atoms	24
No. water molecules	110
<i>R</i> <sub>cryst</sub> (%)	22.8
<i>R</i> <sub>free</sub> (%)	25.0
R.m.s.d. bond lengths (Å)	0.005
R.m.s.d. bond angles (°)	1.0
Average <i>B</i> factor (Å <sup>2</sup> )	33.7

and *SCALEPACK* (Otwinowski & Minor, 1997). The quality of the diffraction data is summarized in Table 1.

### 2.3. Structure determination and refinement

Since the homology between PCM6 and animal CaMs is higher than 89% (Fig. 1), the structure of PCM6 was solved by molecular replacement using the animal CaM structure as the search model. The software we used was *MOLREP* v.7.2 (Vagin & Teplyakov, 1997). In the first attempt, the whole molecule of 3cln (CaM from *Rattus rattus*) was chosen as the search model, but this attempt failed. CaM molecules are dumbbell-shaped, consisting of two lobes connected by a long central helix. A conformational change in the central helix could greatly affect the overall conformation of the molecule while the conformation of the two lobes remain stable. Therefore, the N-lobe (residues 7–71) and C-lobe (residues 80–144) of 3cln were used separately as search models. Both models produced promising results, but these overlapped each other. This is because the conformation of the two lobes is very similar (the r.m.s.d. on C $\alpha$  superposition between residues 7–71 and residues 80–144 of 3cln is only 0.93 Å calculated using *O*; Jones *et al.*, 1991), so that taking either one as the model will result in almost the same solution as the other. In order to clarify which solution is correct, two schemes were tried: fixing the rotation and translation solution of the N-lobe in order to search for the C-lobe, or fixing

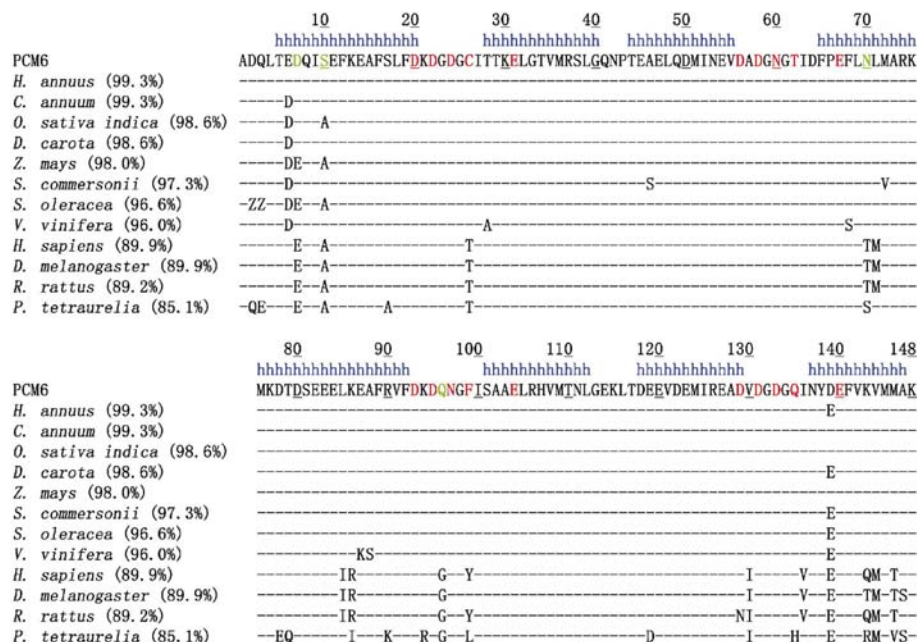


**Figure 1**

Sequence alignment of CaMs from plants, animals and *P. tetraurelia*. CaMs from higher plants: PCM6, *Helianthus annuus*, *Capsicum annuum*, *Oryza sativa indica*, *Daucus carota*, *Zea mays*, *Solanum commersonii*, *Spinacea oleracea*, *Vitis vinifera*. CaMs from higher animals: *Homo sapiens*, *Drosophila melanogaster*, *Rattus rattus*. CaM from protozoa: *P. tetraurelia*. Amino acids are indicated in single-letter IUPAC nomenclature. Dashes indicate identical residues compared with the PCM6 sequence; the sequence identity is given in parentheses. Red letters indicate the residues that contribute to the coordination of the calcium ion. The unique residues in PCM6 (compared with animal CaM sequences) that contribute to the intermolecular interactions in the crystal structure are indicated by green letters. Residues belonging to the seven  $\alpha$ -helices are indicated by a blue 'h'.

the rotation and translation solution of the C-lobe in order to search for the N-lobe. The second scheme resulted in better statistics ( $CC = 0.32$  as opposed to  $0.279$ ) and it gave the solutions of both lobes in such a way that they could form a whole CaM molecule, indicating that the second scheme should be correct. To further test its correctness, we combined the solutions (PDB files already created using *MOLREP*) of the two lobes into a new 'molecule'. A molecular-replacement search using this new model resulted in a good solution ( $R = 0.495$ ,  $CC = 0.449$ ), which exactly overlapped the model itself, and the packing state of the molecules was reasonable. This provided clear proof that the second scheme was correct.

In order to reduce bias and build the missing residues, the starting model (produced by *MOLREP*) was inspected and

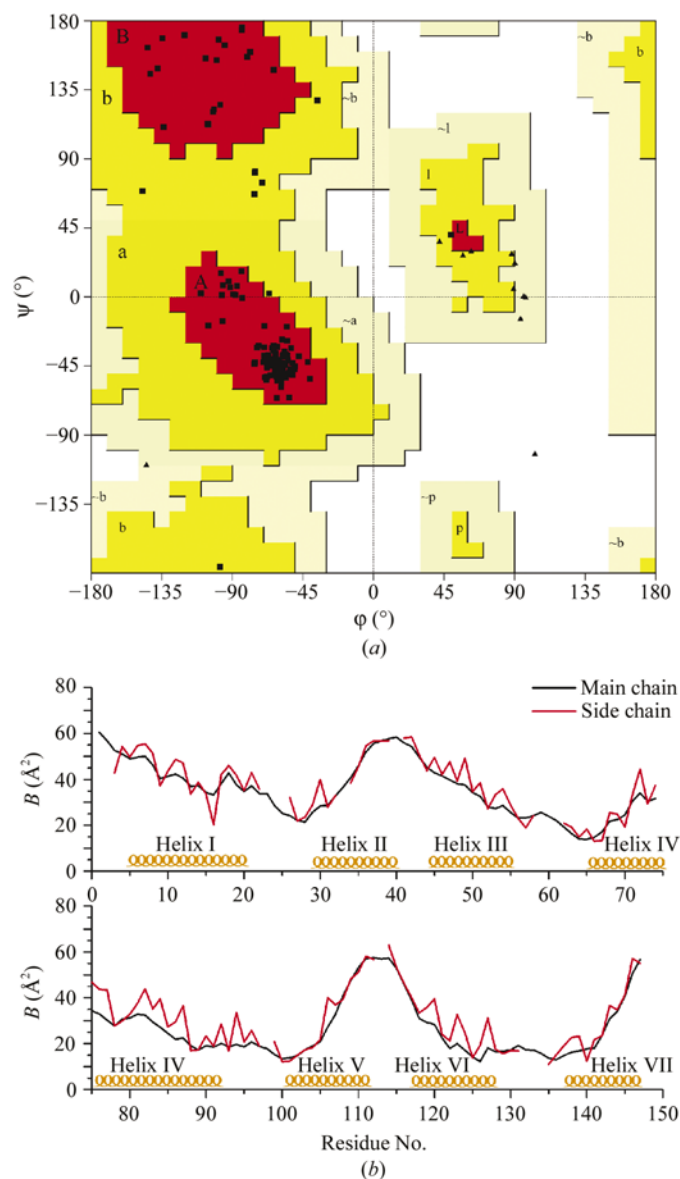


**Figure 2**

Ramachandran plot (Laskowski *et al.*, 1993) and  $B$ -factor distribution of the final model of PCM6. The side chain of Phe16 shows a  $B$  value much lower than that of the main-chain atoms. This is because the side chain of Phe16 is located in a highly hydrophobic core and interacts with several hydrophobic groups (side chains of Phe19, Ile27, Ile63, Phe65 and Phe68), thus stabilizing the phenyl group.

rebuilt against the  $2F_o - F_c$  and  $F_o - F_c$  electron-density maps at  $3.0 \text{ \AA}$  for several runs before refinement, finally resulting in a model containing residues 7–145. The refinement of the PCM6 structure was performed using *CNS* (Brünger *et al.*, 1998); *O* (Jones *et al.*, 1991) was used to manually adjust the structure between the cycles of *CNS* refinement. Some residues were remodelled when necessary. The whole refinement procedure used  $8.0\text{--}2.0 \text{ \AA}$  diffraction data. The details of the refinement are summarized in Table 1.

### 3. Results and discussions

#### 3.1. Quality of the final model

*CNS* (Brünger *et al.*, 1998) and *PROCHECK* (Laskowski *et al.*, 1993) were used to check the quality of the final refined model. The final crystallographic  $R$  factor was  $22.8\%$  and the  $R_{\text{free}}$  factor was  $25\%$ . The r.m.s.d. was  $0.005 \text{ \AA}$  for bond-length deviation and  $1.0^\circ$  for bond-angle deviation.  $93.2\%$  of the residues were located in the most favoured regions in the Ramachandran plot, with  $6.8\%$  located in additional allowed regions; none of the non-Gly residues were located in generously allowed regions or disallowed regions (Fig. 2a). No unreasonably close contacts were found in the model. The overall  $B$  factor of the model was  $33.7 \text{ \AA}^2$  and the  $B$ -factor distribution is shown in Fig. 2(b).

#### 3.2. PCM6 structure

The overall structure of PCM6 is similar to other CaM structures. It is dumbbell-like, consisting of an N-lobe, a C-lobe and a long bent central helix. There are a total of seven  $\alpha$ -helices connected by four  $\text{Ca}^{2+}$ -binding loops and two outstretched loops, which form four EF-hand motifs. Like the other calmodulins, the structure of the two lobes of PCM6 are very similar to each other and can be superimposed on each other with an r.m.s.d. of  $0.89 \text{ \AA}$  ( $C^\alpha$  superposition between residues 12–71 and 85–144).

The calcium-binding peptide contains 12 residues: Asp-*X*-Asp-*X*-Asp/Asn-*X*-Xaa-*X*-*X*-*X*-*X*-Glu (the five residues contributing to the coordination of the calcium ion are shown with three-letter abbreviations). Six ligand groups bind to calcium from the main chain or side chains (the side chain carboxyl O atom of the first, third and fifth residue, the backbone carbonyl O atom of the seventh residue and both of the two carboxylate O atoms of the twelfth residue), with an additional water molecule as the seventh ligand.

A hydrophobic patch is formed on the surface of each of the two lobes and within the patch there is a hydrophobic cavity that can hold a hydrophobic group as large as the side chain of tryptophan (Fig. 3). Three Met residues are located in each hydrophobic patch and around the patch there are two clusters of acidic amino-acid residues (Fig. 3).

#### 3.3. Comparison between PCM6 and animal calmodulins

The conformations of animal and *P. tetraurelia* calmodulins are highly similar to each other, but the conformation of PCM6 is quite different (Table 2). However, the main differ-

ence seems to be in the central helix region and the two lobes of PCM6 are very similar to those of other calmodulins ( $C^\alpha$  superposition with 3cln results in an r.m.s.d. of 0.59 Å for residues 7–71 and 0.74 Å for residues 80–144). In fact, the bending direction of the central helix of PCM6 is obviously different from that of animal/*P. tetraurelia* calmodulins (Fig. 4).

Another distinct difference between PCM6 and the other calmodulins is the crystal-packing state or crystal form. All the animal and *P. tetraurelia* calmodulins crystallized in the same crystal form, space group  $P1$ , with similar unit-cell parameters (Babu *et al.*, 1988; Ban *et al.*, 1994; Chattopadhyaya *et al.*, 1992; Rao *et al.*, 1993; Taylor *et al.*, 1991; Wilson & Brünger, 2000), while PCM6 crystallized in a  $P2_12_12_1$  crystal form, although the crystallization conditions were similar. Usually, it is believed that a packing-state change is caused by changes in molecular conformation or surface-charge properties. Based on the sequence alignment of PCM6 with animal/*P. tetraurelia*

**Table 2**

R.m.s.d. of the structural superposition of calmodulins from different species.

$C^\alpha$  superposition (Å) of residues 7–147, calculated using *O* (Jones *et al.*, 1991).

	PCM6	1osa†‡	4cln†	3cln†	1cll†
1osa†‡	2.66	—			
4cln†	2.79	0.63	—		
3cln†	2.67	0.42	0.59	—	
1cll†	2.63	0.36	0.57	0.27	—

† 1osa, from *Paramecium tetraurelia*; 4cln, from *Drosophila melanogaster*; 3cln, from *Rattus rattus*; 1cll, from *Homo sapiens*. ‡ There are three crystal structures of CaM from *Paramecium tetraurelia*: 1clm, 1osa and 1exr. Here, 1osa was taken as a representative.

calmodulins (Fig. 1), we tend to believe that changes in the surface-charge properties cause PCM6 molecules to pack in a manner that is different from the other calmodulins and that

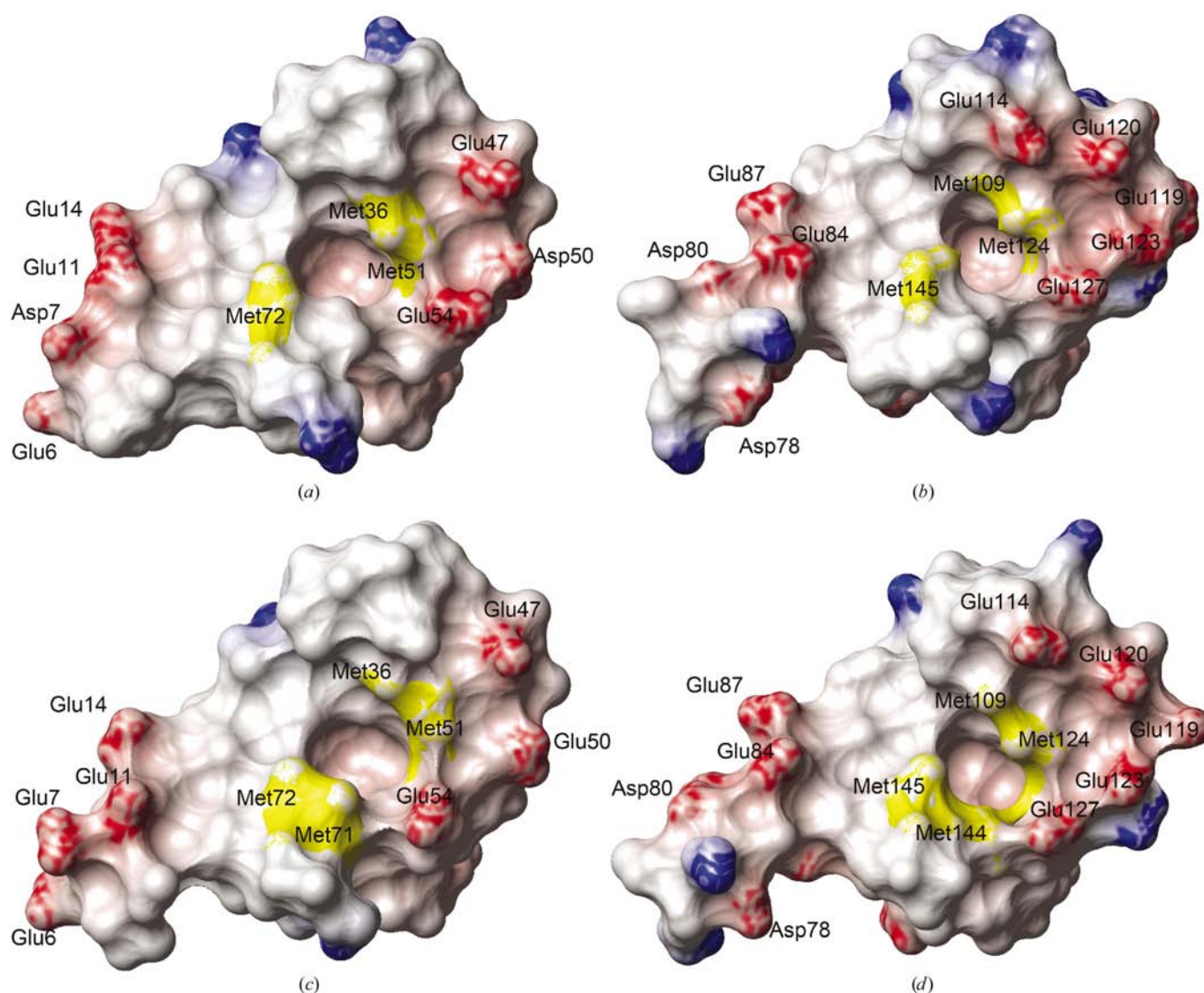


**Figure 3**

Comparison of the hydrophobic patch. (a) N-lobe of PCM6. (b) C-lobe of PCM6. (c) N-lobe of 3cln. (d) C-lobe of 3cln. The grey, red and blue parts indicate the hydrophobic, acidic and basic residues, respectively. The Met residues are coloured yellow. All the acidic residues and Met residues are labelled. This figure was prepared using *MOLMOL* (Koradi *et al.*, 1996).

this different packing style drives the central helix of PCM6 to adopt a different conformation because it is long and relatively flexible. The unique residues (compared with animal calmodulins) Asp7, Ser10, Asn70 and Gln96 were located in

**Table 3**

The polar interactions between neighbouring molecules in the PCM6 crystal that are provided by the unique residues (in bold; compared with animal calmodulins).

Residue	Atom	Interaction distance (Å)	Residue	Atom
<b>Asp7</b>	OD1	3.41	Lys77	NZ
<b>Asp7</b>	OD2	2.45	Lys77	NZ
<b>Asp7</b>	OD2	2.45	Lys77	NZ
<b>Gln96</b>	NE2	2.81	Asp129	OD2
<b>Asn70</b>	OD1	2.82	Gln135	NE2
<b>Asn70</b>	ND2	3.05	Gln135	OE1

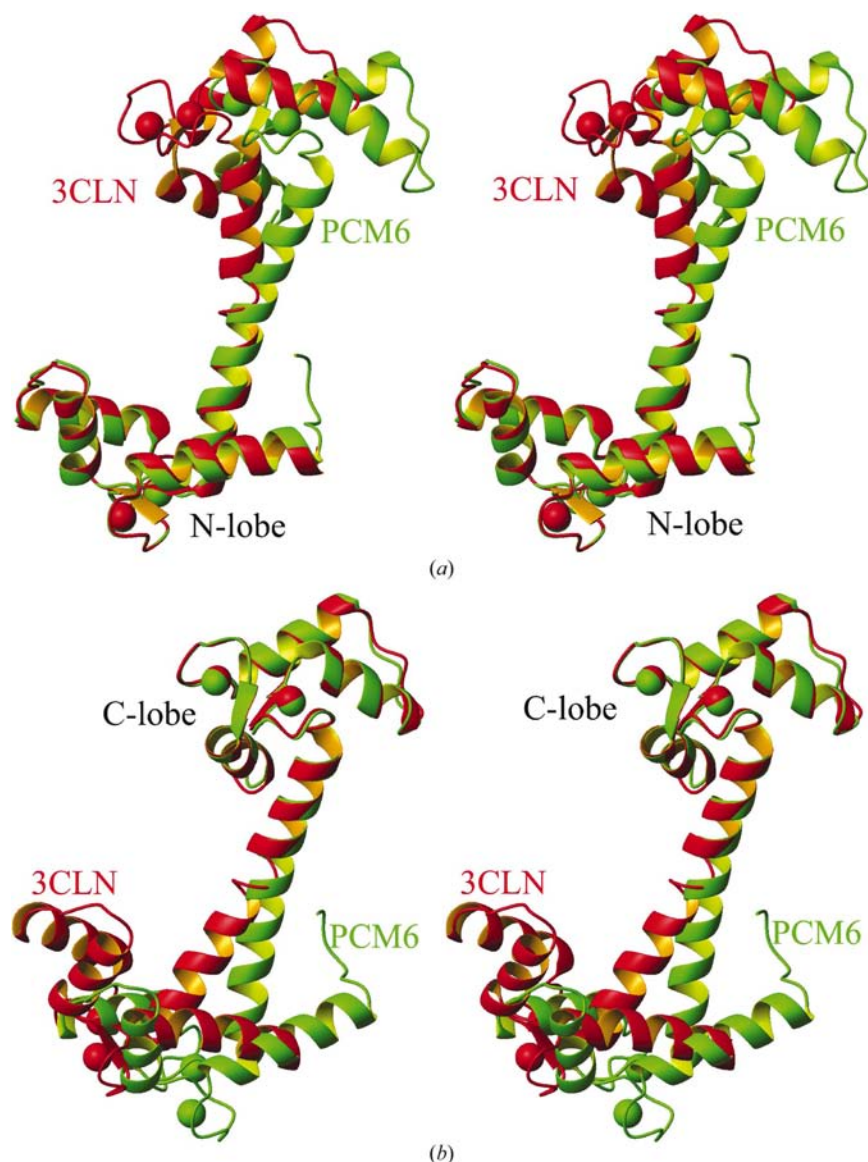


**Figure 4**

Stereoview showing the superposition of PCM6 (green) and 3cln (red). (a) Superposition of the N-lobes. (b) Superposition of the C-lobes. This figure was prepared using *MOLMOL* (Koradi *et al.*, 1996).

the intermolecular interaction surface and formed six polar interactions (Table 3) with neighbouring molecules that are not likely to occur in animal calmodulins (in animal calmodulins these residues are Glu7, Ala10, Thr70 and Gly96, of which only the first tends to make polar interaction with other residues). Although four residues in the central helix region of PCM6 (Asn70, Leu71, Leu85 and Lys86) were different from those in animal calmodulins (Thr70, Met71, Ile85 and Arg86), we tend to believe that this is not the main reason for the conformational change, as the side chains of these residues stretch out into the solvent region, showing no remarkable interactions with other residues, and their charge properties are similar (Asn compared with Thr, Leu with Met or Ile and Lys with Arg).

The hydrophobic patches are very important for target-peptide binding by CaM. According to the model of the animal CaM–target complex, the hydrophobic patches along with the acidic clusters are responsible for the target binding of CaM. The target peptide is usually a basic amphiphilic helix, which contains hydrophobic residues on one side and basic residues on the other, and there is often a residue with a large hydrophobic side chain (*e.g.* Trp, Phe) located at one or both ends of the helix (O’Neil & DeGrado, 1990). The hydrophobic patch of CaM can interact with the hydrophobic side of the target peptide, holding the large hydrophobic side chain of the peptide in the hydrophobic hole to anchor the target peptide (Ikura, Kay *et al.*, 1991; Ikura, Clore *et al.*, 1992; Meador *et al.*, 1992; O’Neil & DeGrado, 1990) and the acidic clusters of CaM then interact with the basic side of the target peptide (Craig *et al.*, 1987; Weber *et al.*, 1989). The main difference in this part between PCM6 and animal calmodulins is the number of Met residues. The Met residues have been proposed to be important in the adaptation of CaM to different kinds of target peptides, as their long unbranched side chains can undergo certain conformational changes to best fit the shape and nature of the target peptide (Ikura, Clore *et al.*, 1992; Kurokawa *et al.*, 2001). Four Met residues around each of the hydrophobic patches (Met36, Met51, Met71 and Met72 around the hydrophobic patch on the N-lobe and Met109, Met124, Met144 and Met145 around the hydrophobic patch on the C-lobe) were found to be highly conserved in animal calmodulins. However, in PCM6, as in most of the other plant calmodulins, there are only three Met residues in each hydrophobic patch (Fig. 1): Met36, Met51, Met72 and Met109, Met124, Met145. The absence of the third Met

(Met71 and Met144) might have some biological effect on calmodulin function as it changes the structural characteristics of the hydrophobic patch (Fig. 3).

We thank Professor B. W. Poovaiah for providing us with the plasmid containing the PCM6 gene. We also thank Dr Tao Jiang for helpful discussion. This project was financially supported by the National High Technology Research and Development Program (No. 2002BA711A12), the National Natural Science Foundation of China Grants (No. 30130080), the Chinese Academy of Sciences Grants (No. KSCX1-SW-17) and the National Basic Research Program of China (No. 2002CB713801).

## References

- Babu, Y. S., Bugg, C. E. & Cook, W. J. (1988). *J. Mol. Biol.* **204**, 191–204.
- Babu, Y. S., Sack, J. S., Greenhough, T. J., Bugg, C. E., Means, A. R. & Cook, W. J. (1985). *Nature (London)*, **315**, 37–40.
- Ban, C., Ramakrishnan, B., Ling, K. Y., Kung, C. & Sundaralingam, M. (1994). *Acta Cryst.* **D50**, 50–63.
- Biro, R. L., Sun, D. Y., Serlin, B. S., Terry, M. E., Datta, N., Sopory, S. K. & Roux, S. J. (1984). *Plant Physiol.* **75**, 382–386.
- Brünger, A. T., Adams, P. D., Clore, G. M., DeLano, W. L., Gros, P., Grosse-Kunstleve, R. W., Jiang, J.-S., Kuszewski, J., Nilges, M., Pannu, N. S., Read, R. J., Rice, L. M., Simonson, T. & Warren, G. L. (1998). *Acta Cryst.* **D54**, 905–921.
- Chattopadhyaya, R., Meador, W. E., Means, A. R. & Quirocho, F. A. (1992). *J. Mol. Biol.* **228**, 1177–1192.
- Craig, T. A., Watterson, D. M., Prendergast, F. G., Haiech, J. & Roberts, D. M. (1987). *J. Biol. Chem.* **262**, 3278–3284.
- Drum, C. L., Yan, S. Z., Bard, J., Shen, Y. Q., Lu, D., Soelaiman, S., Grabarek, Z., Bohm, A. & Tang, W. J. (2002). *Nature (London)*, **415**, 396–402.
- Elshorst, B., Hennig, M., Forsterling, H., Diener, A., Maurer, M., Schulte, P., Schwalbe, H., Griesinger, C., Krebs, J., Schmid, H., Vorherr, T. & Carafoli, E. (1999). *Biochemistry*, **38**, 12320–12332.
- Ikura, M., Barbato, G., Klee, C. B. & Bax, A. (1992). *Cell Calcium*, **13**, 391–400.
- Ikura, M., Clore, G. M., Gronenborn, A. M., Zhu, G., Klee, C. B. & Bax, A. (1992). *Science*, **256**, 632–638.
- Ikura, M., Kay, L. E., Krinks, M. & Bax, A. (1991). *Biochemistry*, **30**, 5498–5504.
- Ikura, M., Spera, S., Barbato, G., Kay, L. E., Krinks, M. & Bax, A. (1991). *Biochemistry*, **30**, 9216–9228.
- James, P., Vorherr, T. & Carafoli, E. (1995). *Trends Biochem. Sci.* **20**, 38–42.
- Jones, T. A., Zou, J. Y., Cowan, S. W. & Kjeldgaard, M. (1991). *Acta Cryst.* **A47**, 110–119.
- Koradi, R., Billeter, M. & Wuthrich, K. (1996). *J. Mol. Graph.* **14**, 51–55.
- Kurokawa, H., Osawa, M., Kurihara, H., Katayama, N., Tokumitsu, H., Swindells, M. B., Kainosho, M. & Ikura, M. (2001). *J. Mol. Biol.* **312**, 59–68.
- Laskowski, R. A., MacArthur, M. W., Moss, D. S. & Thornton, J. M. (1993). *J. Appl. Cryst.* **26**, 283–291.
- Meador, W. E., Means, A. R. & Quirocho, F. A. (1992). *Science*, **257**, 1251–1255.
- O’Neil, K. T. & DeGrado, W. F. (1990). *Trends Biochem. Sci.* **15**, 59–64.
- Osawa, M., Tokumitsu, H., Swindells, M. B., Kurihara, H., Orita, M., Shibamura, T., Furuya, T. & Ikura, M. (1999). *Nature Struct. Biol.* **6**, 819–824.
- Otwinowski, Z. & Minor, W. (1997). *Methods Enzymol.* **276**, 307–326.
- Rao, S. T., Wu, S., Satyshur, K. A., Ling, K. Y., Kung, C. & Sundaralingam, M. (1993). *Protein Sci.* **2**, 436–447.
- Schumacher, M. A., Rivard, A. F., Bachinger, H. P. & Adelman, J. P. (2001). *Nature (London)*, **410**, 1120–1124.
- Taylor, D. A., Sack, J. S., Maune, J. F., Beckingham, K. & Quirocho, F. A. (1991). *J. Biol. Chem.* **266**, 21375–21380.
- Vagin, A. & Teplyakov, A. (1997). *J. Appl. Cryst.* **30**, 1022–1025.
- Weber, P. C., Lukas, T. J., Craig, T. A., Wilson, E., King, M. M., Kwiatkowski, A. P. & Watterson, D. M. (1989). *Proteins*, **6**, 70–85.
- Wilson, M. A. & Brünger, A. T. (2000). *J. Mol. Biol.* **301**, 1237–1256.
- Zielinski, R. E. (1998). *Annu. Rev. Plant Physiol. Plant Mol. Biol.* **49**, 697–725.